

Re-epithelialization of whole porcine kidneys with renal epithelial cells

Journal of Tissue Engineering
Volume 8: 1–11
© The Author(s) 2017
Reprints and permissions:
sagepub.co.uk/journalsPermissions.nav
DOI: 10.1177/2041731417718809
journals.sagepub.com/home/tej



Nafiseh Poornejad¹, Evan Buckmiller², Lara Schaumann¹, Haonan Wang³, Jonathan Wisco⁴, Beverly Roeder⁵, Paul Reynolds⁴ and Alonzo Cook¹

Abstract

Decellularized porcine kidneys were recellularized with renal epithelial cells by three methods: perfusion through the vasculature under high pressure, perfusion through the ureter under high pressure, or perfusion through the ureter under moderate vacuum. Histology, scanning electron microscopy, confocal microscopy, and magnetic resonance imaging were used to assess vasculature preservation and the distribution of cells throughout the kidneys. Cells were detected in the magnetic resonance imaging by labeling them with iron oxide. Perfusion of cells through the ureter under moderate vacuum (40 mmHg) produced the most uniform distribution of cells throughout the kidneys.

Keywords

Recellularization, kidney, epithelial cells, organ regeneration, magnetic resonance imaging

Date received: 8 May 2017; accepted: 13 June 2017

Introduction

Chronic kidney disease (CKD) and end-stage renal failure (ESRF) are among the leading causes of mortality worldwide. According to the National Kidney Foundation, in 2013, more than 47,000 Americans died from kidney failure.¹ The only definitive treatment for ESRF is whole kidney transplantation.^{2,3} However, many patients will die while waiting for a kidney transplant, and those patients who are fortunate enough to receive a kidney must remain on immunosuppressive medication for their whole life.⁴ Engineering artificial kidneys with patient-specific cells may eliminate the risk of immune response induction and the need for a donor organ. A promising approach for creating artificial organs is decellularization of allogeneic or xenogeneic organs to clear away all potential immunogens followed by recellularization with patient-specific cells to regenerate whole healthy organs.^{5–7}

Decellularization of rat,^{8–11} porcine,^{12–14} and human^{6,15} kidneys has been reported in the previous literature. However, recellularization of whole intact renal scaffolds remains a challenge due to the complex structure of kidneys and the numerous cell types in renal tissue required for healthy function. At least one layer of endothelial cells

and one layer of epithelial cells are required to get partial filtration—the prominent kidney function.

Re-endothelialization of whole hearts,^{16–18} livers,^{19,20} lungs,^{21,22} and kidneys^{23,24} has been previously reported. Although it remains a major challenge to cover the entire organ's vascular network, re-endothelialization has been studied more than re-epithelialization of the tubules and collecting ducts. In most published studies, endothelial cells were perfused through the organ's vasculature with

¹Department of Chemical Engineering, Brigham Young University, Provo, UT, USA

²Department of Genetics and Biotechnology, Brigham Young University, Provo, UT, USA

³Department of Electrical Engineering, Brigham Young University, Provo, UT, USA

⁴Department of Physiology and Developmental Biology, Brigham Young University, Provo, UT, USA

⁵Department of Biology, Brigham Young University, Provo, UT, USA

Corresponding author:

Alonzo Cook, Department of Chemical Engineering, Brigham Young University, Provo, UT 84602, USA.

Email: cook@byu.edu



controlled flow rate to allow the cells to adhere and grow within the vascular tree.^{23,24} However, re-epithelialization is not as straightforward since there is no specific pathway for perfusion of epithelial cells. Regeneration of cardiac muscle has been achieved by injection of muscle cells directly into the cardiac scaffold,¹⁶ although this method would not be applicable for organs such as the lung and kidney with their complicated structures. In 2013, Song et al.²⁴ reported a novel method for re-epithelialization of whole rat kidneys by creating a trans-renal pressure gradient and introducing cells through the ureter into the intact renal scaffold.

In this study, we decellularized whole human-sized porcine kidneys with our previously developed method and investigated vascular preservation by magnetic resonance imaging (MRI). We also scaled up the previously described re-epithelialization method for rat kidneys, to recellularize porcine kidney scaffolds, and optimized the various procedures.

Materials and methods

Kidney retrieval

Porcine kidneys (n=50) were harvested from slaughter-weight swine at a local abattoir with special care to preserve sufficient lengths of the renal artery. The kidneys were perfused with heparinized 1× phosphate-buffered saline (PBS) solution through a catheterized renal artery. Subsequently, the harvested organs were preserved at -20°C until decellularization.

Decellularization of whole porcine kidneys

The kidneys were thawed slowly overnight at 4°C and cannulated with white nylon tubing (Value Plastics MTL5210-1, male Luer-slip to 200 series barbed coupler, 1/16" tube ID, distributed by Nordson MEDICAL, Loveland, CO, USA) through the artery, vein, and ureter. Subsequently, the kidneys were attached to an automated decellularization bioreactor that has been previously described^{25,26} and perfused with 0.5% solution of sodium dodecyl sulfate (SDS) in deionized water (DI) water for 7 h. The perfusate flow rate was low at the beginning of the procedure (10 mL/min) and gradually increased to 35 mL/min while keeping the arterial pressure below 80 mmHg (the natural diastolic pressure of the body). Afterward, the decellularized kidneys were perfused with DI water for 48 h with 10 mL/min flow rate to wash out all residual SDS from the renal extracellular matrix (ECM).

Histology

Biopsies of renal cortex (n=4) were excised from native, decellularized, and recellularized kidneys and fixed in 4% paraformaldehyde (PFA) for 24 h and then partially dehydrated in 30%, 50%, and 70% ethanol before complete

dehydration in a graded alcohol series. Subsequently, samples were immersed in xylene and embedded in paraffin, and 5 µm slices were cut and mounted on slides. The sectioned samples were dehydrated and deparaffinized, and then stained with standard hematoxylin and eosin (H&E; Thermo Scientific, Pittsburgh, PA, USA), Picro-Sirius Red stain (Direct Red 80; Sigma-Aldrich, St Louis, MO, USA; #365548), or Safranin O and Fast Green according to the manufacturer's instructions. Imaging of all stained samples was performed using a standard light microscope equipped with a digital camera (Olympus America Inc., Center Valley, PA, USA) at magnifications of 20× and 40×.

Scanning electron microscopy

Small biopsies (n=5) were taken from the cortex region of native and decellularized kidneys, soaked in 2% glutaraldehyde in Millonig's phosphate buffer (MPB) at pH 7.3 for 24 h at 4°C, and then exposed to a buffer wash with MPB (pH 7.3) on a bench-top shaker. Subsequently, samples were submerged in a cryoprotectant consisting of 25% sucrose and 10% glycerol in a 0.5 M PBS solution for 2 h and fractured under liquid nitrogen. The buffer wash procedure was followed by 1.5 h in a 1% OsO₄, MPB (pH 7.3) solution. Samples were dehydrated inside critical dryer baskets with 70%, 95%, and three steps of 100% ethanol solution baths and dried in a CO₂ critical point dryer and subsequently mounted on aluminum stands. Samples were sputter-coated with 15 nm of a gold-palladium (Au-Pd) alloy and imaged with a scanning electron microscope (Philips/FEI XL30ESEMSEG, Hillsborough, OR, USA).

Labeling canine cells with iron oxide particles

Madin-Darby Canine Kidney (MDCK) epithelial cells (provided by Feinberg School of Medicine, Northwestern University, Chicago, IL, USA) were selected as an inexpensive model cell line for preliminary studies due to their similarity to human renal epithelial cells. The MDCK cells were grown in 1× Dulbecco's Modified Eagle Medium (DMEM; Gibco by Life Technologies, Grand Island, NY, USA) supplemented with 10% fetal bovine serum (FBS; Hyclone, Logan, UT, USA) and 1% Pen-Strep (Gibco by Life Technologies) at 37°C and 5% CO₂ environment. At 70%–80% confluence, the cells were exposed to the cell culture medium containing 20, 40, and 60 µg/mL of magnetic nanoparticles of iron oxide (II, III; #725358, Sigma-Aldrich) for 4 and 24 h. Subsequently, the medium was removed, and the cells were washed with sterile saline solution. The optimum concentration and time exposure were applied for further cell labeling and MRI.

MRI of native and decellularized renal ECM

MR images were acquired on a 3 Tesla Siemens Trio MR scanner (Erlangen, Germany) with a 32-channel head matrix

coil. The multi-slice two-dimensional gradient echo (GRE) sequence was employed to generate the T2* weighted images. The field-of-view (FOV) of the scan was 120mm (readout)×120mm (phase)×1mm (slice), and the acquisition matrix was 512 (readout)×512 (phase encode) and 35 in slices' direction which yielded a voxel size equal to 0.23×0.23×1mm. Eight averages and phase stabilization were applied, and the total acquisition time was about 75 min. The ratio of repetition time to echo time (TR/TE) was 1090/10ms and the flip angle was 25°. The readout bandwidth was 260Hz/pixel, and the slice distance was 0.2mm.

Recellularization bioreactor design and construction

The schematic diagram of the recellularization bioreactor is shown in Figure 1. Two Nalgene wide-mouth straight-sided polymethylpentene (PMP) jars (500 and 1000mL; Thermo Scientific, Waltham, MA, USA) were connected through cannulation on the sidewall. Three white polypropylene adaptors (Value Plastics MTL5210-1, male Luer-slip to 200 series barbed coupler, 1/16" tube ID) were inserted into the cap of the 1000-mL jar (main container) to provide connections for the artery, ureter, and vacuum line. Four filtered caps were also attached to the 500-mL jar to oxygenate the cell culture medium (media container). The main container was equipped with a handheld digital manometer (HHP-100G; OMEGA, Stamford, CT, USA) and connected to a vacuum pump. Two Luer-lock valves were also inserted into the artery and ureter lines of the main container for injection of cells into the renal ECM. Silicone rubber tubing was used to connect the containers to the peristaltic pumps. The adaptors were sealed in place with Stik'n Seal® Outdoor Adhesive and Epoxy Instant Mix™ (Loctite; Henkel Corporation, Westlake, OH, USA). All of the various parts of the system were designed to be sterilized through autoclave and fit in an incubator.

Whole kidney ECM sterilization and preparation for recellularization

After 2 days of washing with DI water, the renal ECMs (n=60) were perfused with a solution of 70% ethanol in autoclaved DI water containing 1% Pen–Strep (Gibco by Life Technologies) and 2.5 µg/mL of amphotericin B (Sigma-Aldrich) for 2h in a biosafety cabinet and washed with autoclaved DI water containing antimicrobial agents. Subsequently, the sterile ECM was aseptically moved to the autoclaved bioreactor and was perfused with the cell culture medium at 37°C for at least 2h before introducing cells to the ECM.

Canine kidney cell growth and recellularization of whole renal ECM

MDCK epithelial cells were grown in multi-layer flasks (Nest Scientific, Rahway, NJ, USA) in 1× DMEM (Gibco

by Life Technologies) supplemented with 10% FBS (Hyclone) and 1% Pen–Strep (Gibco by Life Technologies) at 37°C and 5% CO₂ environment. On the day of the experiment, the MDCKs were detached using TrypLE Express (Life Technologies), Grand Island, NY, USA), and 6±0.5×10⁸ cells were suspended in 120, 60, and 6mL of the cell culture medium depending on the desired concentration of cells for recellularization.

Arterial recellularization. The cell solution was injected through the arterial Luer valve through a Luer-lock syringe, and media perfusion was resumed immediately with 70–80mL/min flow rate and continued for 30min. Subsequently, the media perfusion was continued for 7 days at 5mL/min flow rate in an incubator at 37°C and 5% CO₂ environment.

Ureteral recellularization with high positive pressure. The cell solution was injected through the ureteral Luer valve through a Luer-lock syringe, and medium was perfused through the ureter at 40mL/min flow rate for 30min. Subsequently, arterial perfusion of the cell culture medium was resumed at 5mL/min and was continued for 7 days.

Ureteral recellularization under vacuum. The cell solution was injected through the ureter while the kidney chamber (main bioreactor) was under 140, 70, or 40mmHg vacuum depending on the desired vacuum pressure for each experiment. After cell injection, the vacuum was released, and arterial media perfusion was resumed at 5mL/min and continued for 7 days.

During 7 days of cell growth, the cell culture medium was changed every other day. On day 7, the ECM was removed, and random samples of medulla and cortex regions were excised and prepared for H&E staining as described above.

Cell labeling and three-dimensional imaging of recellularized ECM

The optimized reseeding method was applied using fluorescently labeled MDCKs to track cells in the ECM structure using three-dimensional (3D) imaging. On the day of recellularization, the detached cells were suspended in 1× DMEM (Gibco by Life Technology) containing 5 µM SP-DiOC18 (Life Technologies, Grand Island, NY, USA) and incubated at 37°C for 20min. Subsequently, the cells were washed three times with 1× DMEM and suspended in cell culture medium for recellularization. The recellularization of whole porcine ECM with labeled cells was performed through ureteral injection while 40mmHg vacuum was applied to the kidney chamber. After 7 days of cell growth, random slices of renal cortex and medulla were excised and fixed in 4% PFA overnight. Images of the 3D structure of recellularized ECM were obtained using an Olympus

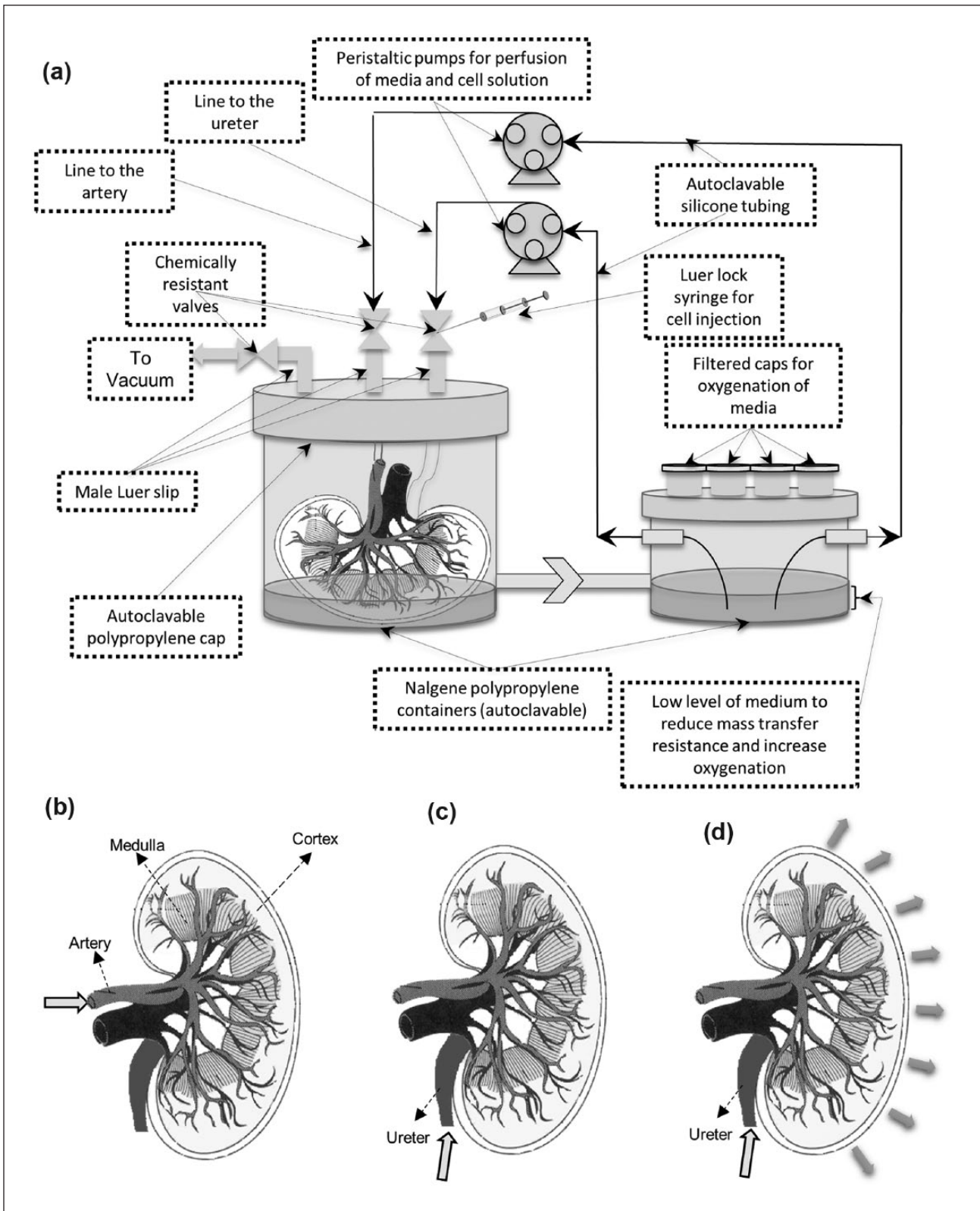


Figure 1. (a) Schematic diagram of whole kidney scaffold recellularization; reseeding procedure: (b) arterial injection of cells with high flow rate or high positive pressure, (c) ureteral injection of cells with high positive pressure, and (d) ureteral injection of cells while the whole chamber was under vacuum to create a trans-renal pressure gradient through the scaffold.

FluoView™ FV1000 (Center Valley, PA, USA) laser scanning confocal microscope.

Results

Decellularization of whole porcine kidneys

Perfusion decellularization of whole porcine kidneys was performed by a method previously developed in our laboratory.^{25,26} Gross anatomy of native and decellularized kidney scaffolds is shown in Figure 2(a) and (b), respectively. Standard H&E staining confirmed removal of the majority of cellular materials through decellularization while the collagenous structure of the scaffold remained intact (Figure 2(c) and (d)). Picro-Sirius Red stain of native and acellular tissue demonstrated the preservation of collagen fibers throughout the renal tissue. Partial conservation of glycosaminoglycans (GAGs), which are also of vital importance for cellular growth and activity, was verified by Safranin O staining (Figure 2(g) and (h)). Collagen and elastin fibers contributing to ultrastructure and mechanical strength of renal tissue were examined using scanning electron microscopy (SEM) imaging. As shown in Figure 2(i) and (j), no apparent fiber disruption could be detected as a result of chemical decellularization of native renal tissue.

Vasculature investigation using MRI

Native and decellularized porcine kidneys were perfused in either the renal artery (Figure 3(a) and (c)) or proximal ureter (Figure 3(b) and (d)) with MDCK cells (1 million cells/mL in a total of 100 mL cell solution for each kidney) that were labeled with iron oxide particles (40 µg/mL). GRE MR images showed the positive location of the cells containing iron oxide. Cells injected into either native (Figure 3(a) and (b)) or decellularized (Figure 3(c) and (d)) kidneys were confined to the spaces corresponding to the perfusion vessel, either in the arterial branches or renal spaces. Cells diffused into the cortical vasculature in the decellularized kidney, whereas cells diffused as far as minor calyces in the urinary space in both native and decellularized kidneys. There was no difference between cell flow through native and decellularized scaffolds confirming vasculature preservation after decellularization.

Preparation of the recellularization bioreactors

Compartments of the recellularization system were autoclaved for 30 min to remove potential sources of microbial contamination. The kidney scaffolds were perfused with 70% ethanol in autoclaved DI water containing 1% Pen-Strep and 2.5 µg/mL amphotericin B. Subsequently, the kidneys were aseptically moved to the bioreactor and perfused with 2 L of autoclaved DI water containing antimicrobial agents to remove residual ethanol from the ECM.

We previously examined the cytotoxicity of ECM to canine MDCKs after sterilization with 70% ethanol.²⁷ The sterile kidneys were perfused with cell culture medium at least for 2 h to rehydrate the ECM and increase the biocompatibility of the ECM.

Optimization of cell seeding to the renal scaffold

Introducing the cells back to the renal scaffold was optimized by changing cell solution concentrations and seeding methods. A total of 500±100 million cells with concentrations of 1×10^8 , 1×10^7 , and 5×10^6 cells/mL were perfused or injected through the renal ureter. We observed that the lower concentrations of cells resulted in more homogeneous distribution of cells throughout the kidney. High concentrations of cells led to cell clot formation in tubules of the medulla region without any cells reaching the cortex region. The optimum concentration of cells was found to be 4–5 million cells/mL of culture medium for all applied seeding methods.

In the first trial, the kidneys were arterially perfused (Figure 1(b)) with cell solutions at high flow rate (80–100 mL/min) for 20 min with the hypothesis of forcing the cells into the tubules by pushing them through the vessel's basement membranes. Subsequently, arterial perfusion with oxygenated cell culture media was resumed at a low flow rate (2 mL/min) to avoid washing the cells out of the ECM while providing nutrients and oxygen for the viable cells. After 24 h, the culture media flow rate was increased to 10 mL/min and continued for 7 days. The H&E staining of the recellularized kidneys (Figure 4(a) and (b)) demonstrated that a high flow rate and, consequently, high pressure did not push the cells into the tubules and the majority of the cells remained on the vascular side. In addition, the high flow rate led to the cells washing out from the ECM and only a few cells remained in the glomeruli structure. No cells could be found in the medulla region (Figure 4(a)).

In the second trial, the cells were injected through the ureter with high positive pressure to push the cells all the way to the cortex region and repopulate the tubule side of the kidney (Figure 1(c)). Even at low concentration, the cells remained in the tubules of the medulla with few cells reaching the cortex region (Figure 4(c) and (d)). Since there was no direct output for the high flow rate solution perfusing through the ureter, the pressure became elevated, which could have damaged the cellular membranes.

In the third trial, the cells were injected through the ureter while the whole kidney chamber was under either 40 or 140 mmHg vacuum for 20 min (Figure 1(d)). The H&E staining of resultant recellularized kidneys showed that a majority of the cells were in the cortex region with no cells in the medulla region (Figure 4(e) and (f)). This result demonstrated that the vacuum pressure was the only option to move the cells to the cortex region. However, vacuum

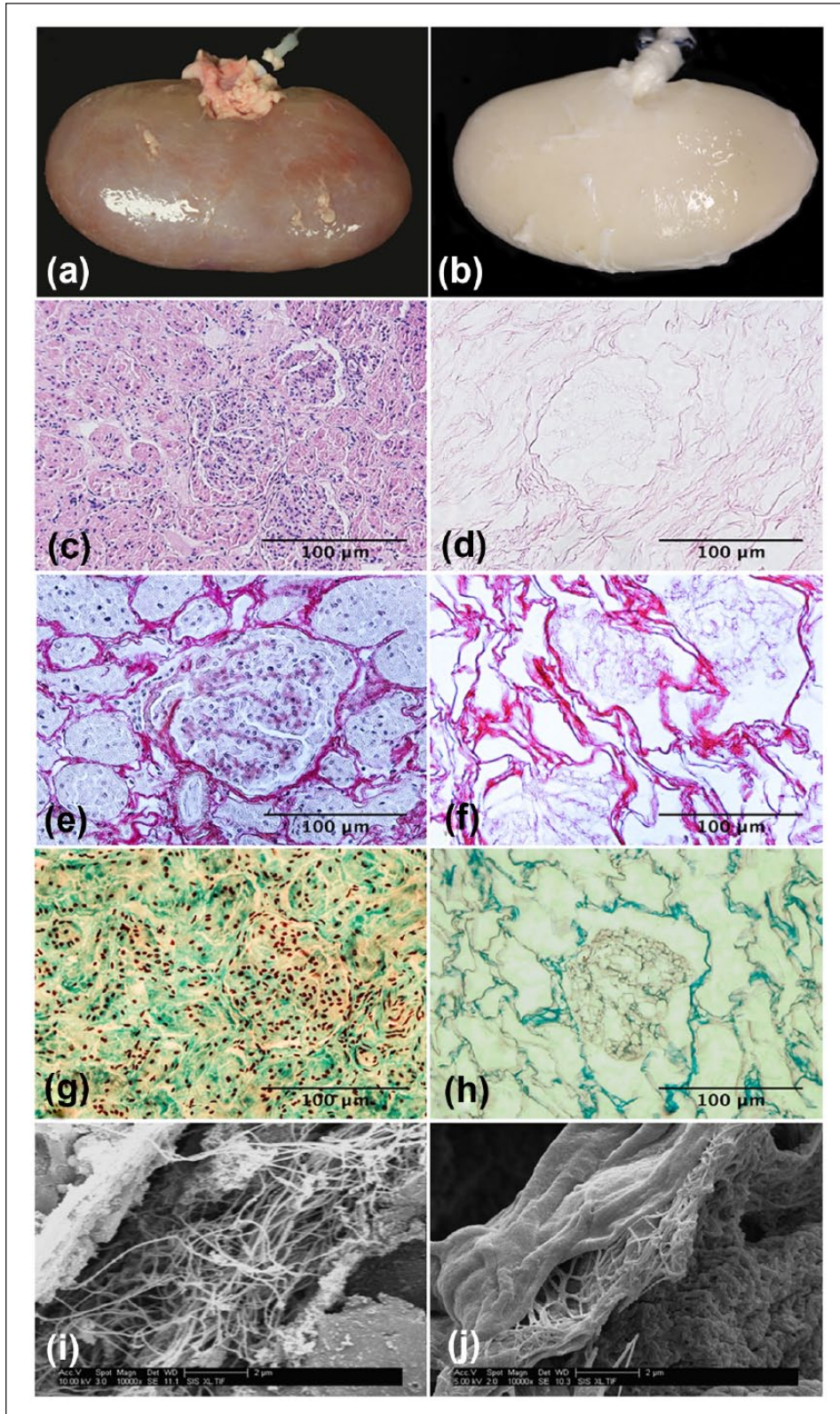


Figure 2. Gross anatomy of (a) native and (b) decellularized whole porcine kidney; standard H&E staining of (c) native and (d) decellularized tissue confirming cell removal through decellularization; Picro-Sirius Red staining of (e) native and (f) decellularized renal tissue demonstrating preservation of collagenous structure of renal tissue through decellularization; Safranin O staining of (g) native and (h) decellularized renal tissue representative of GAGs remaining in the renal tissue structure; and SEM images of (i) native and (j) decellularized renal tissue.

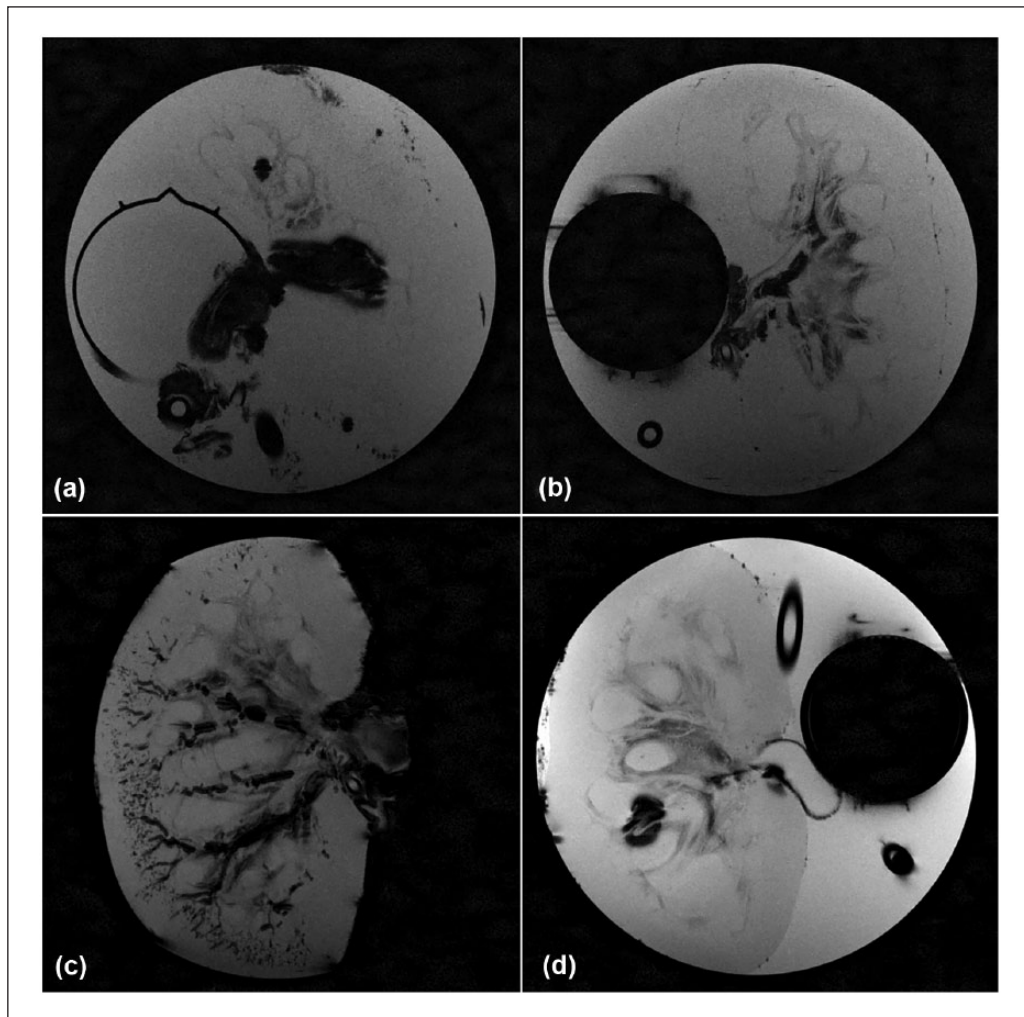


Figure 3. MRI of (a, b) native and (c, d) decellularized porcine scaffold after (a, c) arterial and (b, d) ureteral injections of MDCK cells labeled with iron oxide particles.

pressure should not be too high, and we found that 40 mmHg was the optimum negative pressure for porcine kidneys to repopulate the medulla and cortex regions with minimal cell clotting. As shown in Figure 4(e) and (h), cells lined the tubules in the medulla and cortex regions without cell aggregation.

3D imaging of recellularized kidneys with vacuum method

Canine MDCKs were labeled with fluorescence color before injection through the ureter under 40 mmHg vacuum. After 1 week of cell growth, confocal imaging of thin sections of the renal cortex and medulla was performed, and the resulting images are shown in Figure 5. The thin slices were excised randomly from various regions of renal tissue, and the results showed complete and homogeneous distribution of cells throughout the entire structure, demonstrating survival and good adherence of the cells to the

matrix. In the medulla region, the majority of tubules were repopulated with labeled cells with patent lumens. Imaging of the cortex region demonstrated the presence and growth of renal cells and recellularization of Bowman's capsules with free lumen without signs of cell aggregation. The intact structure of the convoluted tubules could also be observed in the cortex region.

Discussion

Various methods have been proposed to rebuild kidneys.^{5,28,29} The reasons to pursue renal tissue regeneration include the growing waiting list for kidney transplants, poor engraftment of transplanted organs due to immune rejection, and the lifetime need for immunosuppressive medications following transplants. One promising approach to engineer a human-sized kidney without the risk of immune rejection⁴ is the decellularization of a porcine kidney to achieve a perfect matrix for healthy cell

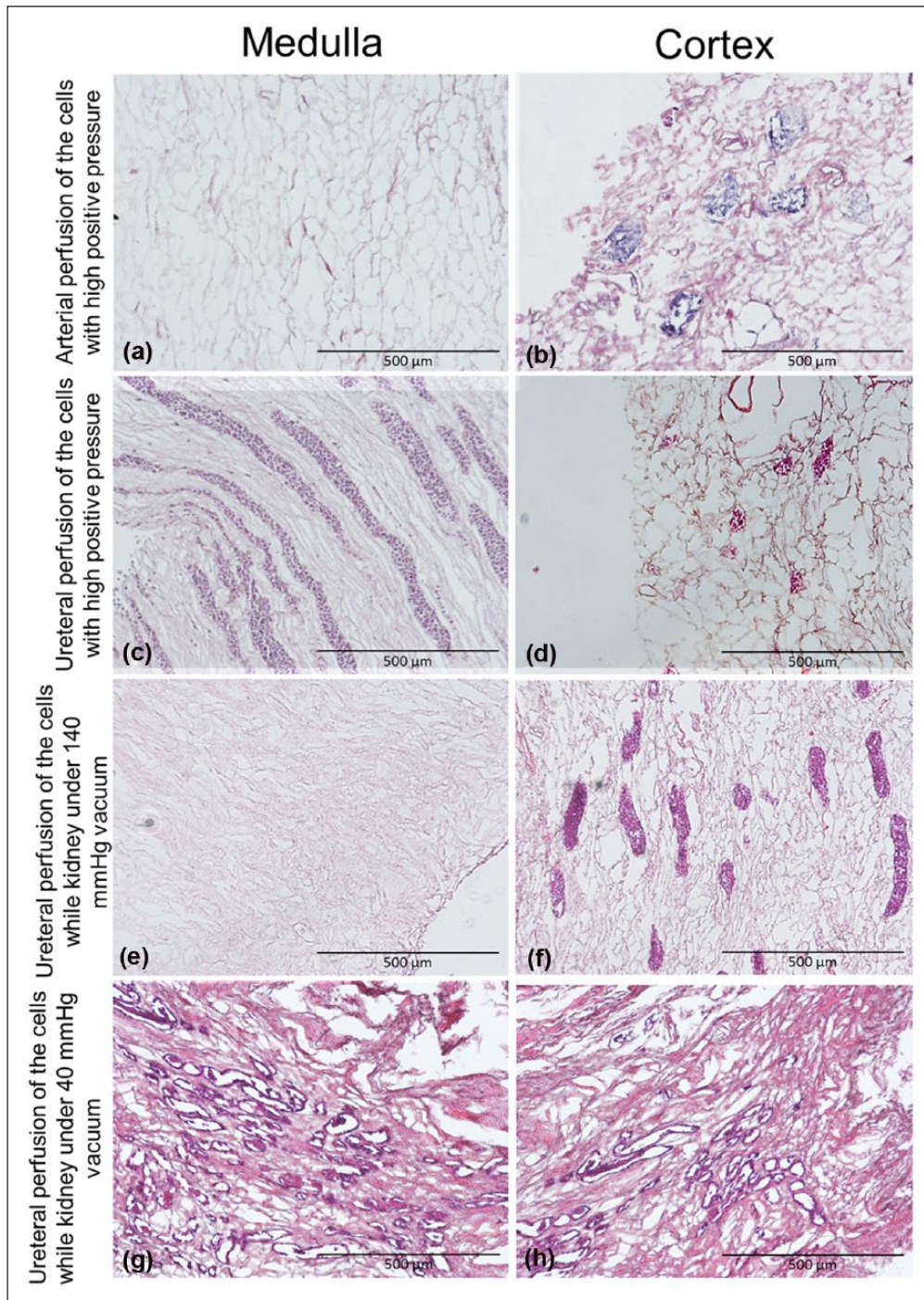


Figure 4. Standard H&E staining of recellularized renal scaffolds in (a, c, e, and g) medullary and (b, d, f, and h) cortical regions 7 days after various seeding methods. Bars represent 500 μm .

growth followed by recellularization of the scaffold by patient-specific human cells. In this study, decellularization of whole porcine kidneys was performed by perfusing detergent through the vascular network to remove most of the cellular materials and potential immunogens to avoid immune response induction at transplantation^{12,25,30,31} We previously optimized and characterized detergents³² and processes²⁶ for whole porcine kidney decellularization and

applied the optimum method in this study. We then recellularized the porcine kidneys with canine renal epithelial cells (as a representative model of xenotransplantation) and characterized the kidneys using histology, SEM, MRI, and confocal microscopy.

One of the fundamental properties of a naturally obtained scaffold is the inherent vascular network, which is critical for healthy organ function.^{6,33} Vascular network

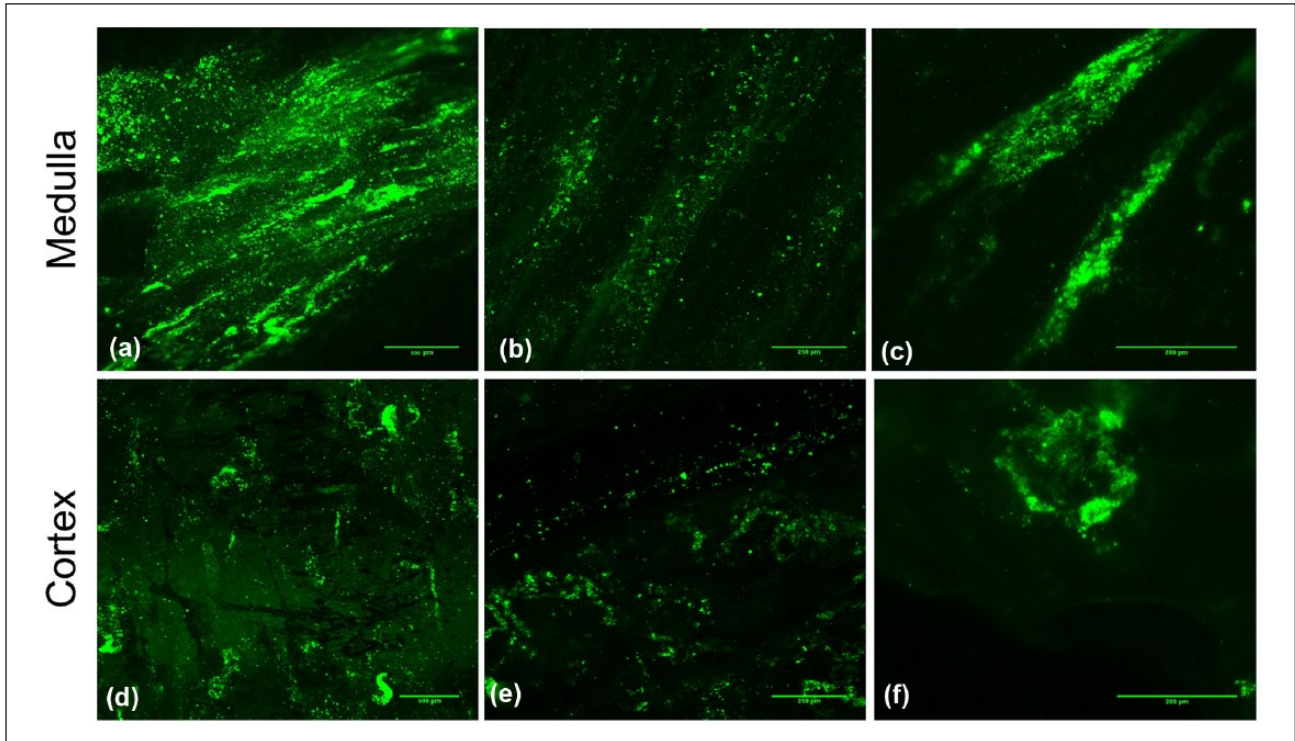


Figure 5. 3D imaging of recellularized kidney 7 days after ureteral injection of fluorescently labeled MDCK cells with trans-renal pressure gradient (40 mmHg vacuum). Bars represent (a and d) 500 μm , (b and e) 250 μm , and (c and f) 200 μm .

intactness of porcine³⁰ and rat³⁴ kidneys after decellularization was previously investigated by computed tomography (CT) imaging and perfusion of fluorescently labeled cells followed by confocal microscopy, respectively. We decided to investigate imaging of decellularized kidneys by MRI. Gadolinium solution is typically used with MRI to get a high-resolution image of the vascular tree; however, we found that gadolinium diffused out of acellular vessel walls due to the lack of an endothelial layer and the relatively small size of gadolinium molecules. Therefore, in this study, MRI images of the vasculature and tubule structures of native and decellularized porcine kidneys were obtained after perfusing the structures with iron oxide–labeled MDCK cells. The labeled cells were injected through the ureter or artery. MDCK cells were not able to diffuse through the vessel walls because of their relatively large size.^{35,36} We labeled the MDCK cells with iron oxide particles to achieve high enough resolution in MRI. The intact vasculature and tubule structures of decellularized scaffolds compared to the native kidney are shown in Figure 3. Cortical capillaries were not detectable for native kidneys due to the relatively large size of cells and lack of diffusion through this region.

Human-sized kidney recellularization introduces several challenges due to the relatively enormous size of the scaffold. Previously, researchers recellularized rat kidneys,^{8,24,34,37,38} to serve as a smaller model of a human-sized kidney. Recently, Ko et al.²³ reported re-endothelialization

of whole piglet kidneys and reconstruction of the vascular tree throughout the renal scaffold. In another study, Abolbashi et al.³⁹ performed re-epithelialization of porcine kidney scaffolds by multiple injections of primary renal cells to the cortical region of renal tissue. They showed partial reconstruction of tubules with limited function of the renal cells compared to a native kidney. However, this method would not be applicable for reconstruction of a whole porcine kidney with complicated structures in the cortical and medullary regions.

In this study, we have scaled up a previously used method for re-epithelialization of rat kidneys and determined the optimum cell concentration and seeding procedures to achieve the homogeneous distribution of cells throughout the whole porcine kidney scaffold. We tested three methods: perfusion through the renal artery under high pressure, perfusion through the ureter under high pressure, and perfusion through the ureter under moderate vacuum. These methods were based, in part, on previous literature. For example, in 2014, Caralt et al. reported re-epithelialization of whole rat kidneys with tubular epithelial cells by perfusion of the cells through the vascular network with high pressure. They showed that high pressure caused the cells to pass through the vessel walls and repopulate the tubule side of the renal structure.³⁴ When we applied this method for whole porcine kidney scaffolds, we found that the majority of cells were washed out from the renal scaffold, and few cells remained in the

capillaries of the glomerulus in the cortex region (Figure 4(a) and (b)). As another example, in 2013, Song et al.²⁴ applied different methods of seeding neonatal kidney cells to rat kidneys and found the ureteral injection of cells using a trans-renal pressure gradient under a vacuum of 40 cmH₂O (30 mmHg) led to the most homogeneous distribution of epithelial cells throughout the entire scaffold.

We confirm herein that a moderate vacuum (40 mmHg) is the most efficient approach for homogeneous distribution of cells through the medullar and cortical regions without resulting in cell blockage (Figure 4(g) and (h)). In future work, we recommend the use of human renal epithelial cells to confirm these results. With human cells, the expression of appropriate renal cell markers and gene expression should be conducted to determine whether there are differential cell–matrix interactions in the various regions of the nephron. Although this study is an important step forward to demonstrate the feasibility of re-endothelialization of porcine kidneys with cells from another species, much additional work is needed to engineer a functional, viable human kidney replacement with all the appropriate cell types located in their proper anatomical locations within the kidney.

Conclusion

This study analyzed three methods for re-epithelialization of whole human-sized kidneys: perfusion through the vasculature under high pressure, perfusion through the ureter under high pressure, or perfusion through the ureter under moderate vacuum and identified the best approach as delivering epithelial cells through the ureter using moderate vacuum of 40 mmHg. The distribution of renal epithelial cells after recellularization was validated by MRI and confocal microscopy. Investigation of the functionality of recellularized kidneys with human cells is the next step to confirm the feasibility of artificial kidney reconstruction through this technique. Additional future studies should be focused on increasing cell coverage, identifying specific renal cell markers and gene expression, and providing the appropriate conditions for the cells to develop functional renal tissue.

Declaration of conflicting interests

The author(s) declared no potential conflicts of interest with respect to the research, authorship, and/or publication of this article.

Funding

The author(s) received no financial support for the research, authorship, and/or publication of this article.

References

- Jiaquan X, Murphy SL, Kochanek KD, et al. Deaths: final data for 2013. *Natl Vital Stat Rep* 2016; 64: 1–118.
- Scarritt ME, Pashos NC and Bunnell BA. A review of cellularization strategies for tissue engineering of whole organs. *Front Bioeng Biotechnol* 2015; 3: 1–17.
- Yamanaka S and Yokoo T. Current bioengineering methods for whole kidney regeneration. *Stem Cells Int* 2015; 2015: 724047.
- Badylak SF, Taylor D and Uygun K. Whole-organ tissue engineering: decellularization and recellularization of three-dimensional matrix scaffolds. *Ann Rev Biomed Eng* 2011; 13: 27–53.
- Moran E, Dhal A, Vyas D, et al. Whole organ bioengineering—current tales of modern alchemy. *Transl Res* 2014; 163: 259–267.
- Katari R, Peloso A, Zambon JP, et al. Renal bioengineering with scaffolds generated from human kidneys. *Nephron Exp Nephrol* 2014; 126: 119.
- Figliuzzi M, Remuzzi G and Remuzzi A. Renal bioengineering with scaffolds generated from rat and pig kidneys. *Nephron Exp Nephrol* 2014; 126: 113.
- Uzarski JS, Bijonowski BM, Wang B, et al. Dual-purpose bioreactors to monitor non-invasive physical and biochemical markers of kidney and liver scaffold recellularization. *Tissue Eng Part C Methods* 2015; 21: 1032–1041.
- Peloso A, Ferrario J, Maiga B, et al. Creation and implantation of acellular rat renal ECM-based scaffolds. *Organogenesis* 2015; 11: 58–74.
- Yu Y, Shao Y, Ding Y, et al. Decellularized kidney scaffold-mediated renal regeneration. *Biomaterials* 2014; 35: 6822–6828.
- Burgkart R, Tron A, Proding P, et al. Decellularized kidney matrix for perfused bone engineering. *Tissue Eng Part C Methods* 2014; 20: 553–561.
- Guan Y, Liu S, Liu Y, et al. Porcine kidneys as a source of ECM scaffold for kidney regeneration. *Mater Sci Eng C Mater Biol Appl* 2015; 56: 451–456.
- Wang Y, Bao J, Wu Q, et al. Method for perfusion decellularization of porcine whole liver and kidney for use as a scaffold for clinical-scale bioengineering engrafts. *Xenotransplantation* 2014; 22: 48–61.
- Park K and Woo H. Porcine bioengineered scaffolds as new frontiers in regenerative medicine. *Transplant Proc* 2012; 44: 1146–1150.
- Orlando G, Booth C, Wang Z, et al. Discarded human kidneys as a source of ECM scaffold for kidney regeneration technologies. *Biomaterials* 2013; 34: 5915–5925.
- Ott HC, Matthiesen TS, Goh SK, et al. Perfusion-decellularized matrix: using nature's platform to engineer a bioartificial heart. *Nat Med* 2008; 14: 213–221.
- Lu T-Y, Lin B, Kim J, et al. Repopulation of decellularized mouse heart with human induced pluripotent stem cell-derived cardiovascular progenitor cells. *Nat Commun* 2013; 4: 1–14.
- Robertson MJ, Dries-Devlin JL, Kren SM, et al. Optimizing recellularization of whole decellularized heart extracellular matrix. *PLoS ONE* 2014; 9: e90406.
- Uygun BE, Soto-Gutierrez A, Yagi H, et al. Organ reengineering through development of a transplantable recellularized liver graft using decellularized liver matrix. *Nat Med* 2010; 16: 814–820.
- Bao J, Shi Y, Sun H, et al. Construction of a portal implantable functional tissue-engineered liver using perfusion-decellularized matrix and hepatocytes in rats. *Cell Transplant* 2011; 20: 753–766.
- Daly AB, Wallis JM, Borg ZD, et al. Initial binding and recellularization of decellularized mouse lung scaffolds

- with bone marrow-derived mesenchymal stromal cells. *Tissue Eng Part A* 2011; 18: 1–16.
22. Ott HC, Clippinger B, Conrad C, et al. Regeneration and orthotopic transplantation of a bioartificial lung. *Nat Med* 2010; 16: 927–933.
 23. Ko IK, Abolbashari M, Huling J, et al. Enhanced re-endothelialization of acellular kidney scaffolds for whole organ engineering via antibody conjugation of vasculatures. *Technology* 2014; 2: 243–253.
 24. Song JJ, Guyette JP, Gilpin SE, et al. Regeneration and experimental orthotopic transplantation of bioengineered kidney. *Nat Med* 2013; 19: 646–656.
 25. Poornejad N, Frost TS, Scott DR, et al. Freezing/thawing without cryoprotectant damages native but not decellularized porcine renal tissue. *Organogenesis* 2015; 11: 30–45.
 26. Poornejad N, Momtahan N, Salehi ASM, et al. Efficient decellularization of whole porcine kidneys improves reseeded cell behavior. *Biomed Mater* 2016; 11: 025003.
 27. Poornejad N, Nielsen JJ, Morris RJ, et al. Comparison of four decontamination treatments on porcine renal decellularized extracellular matrix structure, composition, and support of human renal cortical tubular epithelium cells. *J Biomater Appl* 2015; 30: 1154–1167.
 28. Poornejad N, Schaumann LB, Buckmiller EM, et al. Current cell-based strategies for whole kidney regeneration. *Tissue Eng Part B Rev* 2016; 30: 1154–1167.
 29. Zambon JP, Magalhaes RS, Ko I, et al. Kidney regeneration: where we are and future perspectives. *World J Nephrol* 2014; 3: 24–30.
 30. Sullivan DC, Mirmalek-Sani S-H, Deegan DB, et al. Decellularization methods of porcine kidneys for whole organ engineering using a high-throughput system. *Biomaterials* 2012; 33: 7756–7764.
 31. Orlando G, Farney AC, Iskandar SS, et al. Production and implantation of renal extracellular matrix scaffolds from porcine kidneys as a platform for renal bioengineering investigations. *Ann Surg* 2012; 256: 363–370.
 32. Poornejad N, Schaumann LB, Buckmiller EM, et al. The impact of decellularization agents on renal tissue extracellular matrix. *J Biomater Appl* 2016; 31: 521–533.
 33. Zambon J, Ko I, Abolbashari M, et al. Optimization of porcine kidney decellularization methods for long-term implantation. *Tissue Eng Part A* 2015; 21: S162–S163.
 34. Caralt M, Uzarski JS, Iacob S, et al. Optimization and critical evaluation of decellularization strategies to develop renal extracellular matrix scaffolds as biological templates for organ engineering and transplantation. *Am J Transplant* 2014; 15: 64–75.
 35. Will S, Martirosian P, Eibofner F, et al. Viability and MR detectability of iron labeled mesenchymal stem cells used for endoscopic injection into the porcine urethral sphincter. *NMR Biomed* 2015; 28: 1049–1058.
 36. Kim SJ, Lewis B, Steiner MS, et al. Superparamagnetic iron oxide nanoparticles for direct labeling of stem cells and in vivo MRI tracking. *Contrast Media Mol Imaging* 2016; 11: 55–64.
 37. Bonandrini B, Figliuzzi M, Papadimou E, et al. Recellularization of well-preserved acellular kidney scaffold using embryonic stem cells. *Tissue Eng Part A* 2014; 20: 1486–1498.
 38. Ross EA, Abrahamson DR, St John P, et al. Mouse stem cells seeded into decellularized rat kidney scaffolds endothelialize and remodel basement membranes. *Organogenesis* 2012; 8: 49–55.
 39. Abolbashari M, Agcaoili SM, Lee MK, et al. Repopulation of porcine kidney scaffold using porcine primary renal cells. *Acta Biomater* 2016; 29: 52–61.